Cancer Immunology, Immunotherapy (2019) 68:907–915
https://doi.org/10.1007/s00262-019-02323-x

ORIGINAL ARTICLE

DNA lesions correlate with lymphocyte function after selective internal radiotherapy

Aglaia Domouchtsidou[1] · Vahé Barsegian[2] · Stefan P. Mueller[3] · Pavel Lobachevsky[4] · Jan Best[5,6] · Peter A. Horn[1] · Andreas Bockisch[3] · Monika Lindemann[1]

Received: 28 September 2018 / Accepted: 11 March 2019 / Published online: 15 March 2019

Abstract

In patients with non-resectable hepatic malignancies selective internal radiotherapy (SIRT) with yttrium-90 is an effective therapy. However, previous data indicate that SIRT leads to impaired immune function. The aim of the current study was to determine the extent of DNA lesions in peripheral blood mononuclear cells of SIRT patients and to correlate these lesions with cellular immune responses. In ten patients γH2AX and 53BP1 foci were determined. These foci are markers of DNA double-strand breaks (DSBs) and occur consecutively. In parallel, lymphocyte proliferation was assessed after stimulation with the T cell mitogen phytohemagglutinin. Analyses of vital cells were performed prior to and 1 h and 1 week after SIRT. 1 h and 1 week after SIRT numbers of γH2AX and of 53BP1 foci were more than threefold larger than before ($p < 0.01$). Already at baseline, foci were more abundant than published in healthy controls. Lymphocyte proliferation at baseline was below the normal range and further decreased after SIRT. Prior to therapy, there was an inverse correlation between lymphocyte proliferation and the quotient 53BP1/γH2AX; which could be considered as a measure of the course of DNA DSB repair ($r = -0.94$, $p < 0.0001$). Proliferative responses were inversely correlated with 53BP1 foci prior to therapy and γH2AX and 53BP1 foci 1 h after therapy ($r < -0.65$, $p < 0.05$). In conclusion, DNA foci in SIRT patients were correlated with impaired in vitro immune function. Unrepaired DNA DSBs or cell cycle arrest due to repair may cause this impairment.

Keywords Selective internal radiotherapy · DNA double strand break · DNA repair · Cellular immune response · Lymphocyte proliferation · ELISpot

This study continues a study published previously (Domouchtsidou A, Barsegian V, Mueller SP, Best J, Ertle J, Bedreli S, et al. Impaired lymphocyte function in patients with hepatic malignancies after selective internal radiotherapy. Cancer Immunol Immunother. 2018;67:843–853).

✉ Monika Lindemann
monika.lindemann@uk-essen.de

1 Institute for Transfusion Medicine, University Hospital Essen, Virchowstraße 179, 45147 Essen, Germany

2 Institute of Nuclear Medicine, Helios Kliniken, Schwerin, Germany

3 Department of Nuclear Medicine, University Hospital, Essen, Germany

4 Advanced Analytical Technologies, Melbourne, Australia

5 Department of Gastroenterology and Hepatology, University Hospital, Essen, Germany

6 Department of Gastroenterology, Hepatology and Infectious Diseases, Otto-von-Guericke-University Magdeburg, Magdeburg, Germany

Abbreviations

DSB	Double strand break
LTT	Lymphocyte transformation test
H2AX	Protein histone 2A family member X
SIRT	Selective internal radiotherapy
53BP1	Tumor suppressor p53-binding protein 1
^{90}Y	Yttrium-90

Introduction

Selective internal radiotherapy (SIRT) with the beta emitter yttrium-90 (^{90}Y) is an effective therapy in patients with non-resectable hepatic malignancies, providing favorable outcomes with minimal side effects [1]. Microspheres labeled with ^{90}Y are injected into the hepatic arteries of tumor-bearing liver segments, lobes or the entire liver. These glass microspheres are irreversibly trapped in the capillaries and irradiate the surrounding tissue until the isotope is decayed (physical half-life 64.1 h). Tumors treatable by SIRT have

higher arterial perfusion than the surrounding tumor-free liver tissue [1]. The average range in tissue of the beta radiation of ^{90}Y is 2.5 mm, the maximum range 11 mm [2]. Since usually no microspheres circulate systemically, outside of the target volume only blood cells are irradiated during their passage through the liver [3]. The prescribed activity of ^{90}Y glass microspheres is based on the average dose to the target volume, i.e. the volume of tissue supplied by the hepatic artery where the microspheres are injected [4]. Usually, the dose to the target volume is 100–120 Gy [5].

It is now generally accepted that tumor-immune cell interactions are highly relevant for patient survival and evidence suggests that in the near future local therapies (e.g., SIRT) may be successfully combined with cancer immunotherapies targeting immune-checkpoint receptors [6–11]. In autumn 2017 a multicenter study on SIRT patients treated with the anti-PD-1 agent nivolumab was started (ClinicalTrials.gov Identifier: NCT03380130). It was hypothesized that the systemic action of nivolumab combined with the local high radiation dose to the liver by SIRT could pose a more effective treatment option. In a recent paper, we described that SIRT leads to an impairment of cellular immune function [12]. Thus, counter-acting the immunosuppressive effect of SIRT by immunotherapy may lead to improved tumor control.

In the current project, we further elucidated immune function in patients with non-resectable hepatic malignancies. We hypothesized that DNA lesions known to occur after irradiation [13] may lead to the impaired cellular immune responses after SIRT. Among different kinds of DNA lesions, in mammalian cells double strand breaks (DSBs) are considered as the most deleterious events after irradiation [14]. Following DNA DSBs, the protein histone 2A family member X (H2AX) is rapidly phosphorylated by protein kinases [15] producing a signaling cascade during which the phosphorylated H2AX molecules (γH2AX) form nuclear foci around the DSBs and lead—via several mediators—to an accumulation of the tumor suppressor p53 binding protein 1 (53BP1) [16]. γH2AX foci co-localize with foci of 53BP1 [17] and can be visualized by immunofluorescence [13, 15, 18]. The different functions of 53BP1 in DNA damage response and repair were recently summarized in a review [16]. 53BP1 recruits additional DNA DSB signaling and repair proteins to the site of DNA damage and promotes ataxia-telangiectasia mutated (ATM)-dependent checkpoint signaling, especially at low levels of DNA damage. Moreover, 53BP1 is a key player in DSB repair pathway choice. It promotes the synapsis of distal DNA ends during non-homologous end-joining. Thus, 53BP1 protects genomic stability by regulating the DNA damage response [16, 19].

At present, no data on γH2AX and 53BP1 foci and cellular immune function after SIRT are available. Therefore, it was the aim of the current study to determine the extent of DNA lesions in vital PBMC of SIRT patients and to correlate these lesions with cellular immune responses. To assess cellular immunity, we measured lymphocyte proliferation and the production of the pro-inflammatory cytokine IFN-γ after stimulation of PBMC with a T cell mitogen. Sequential analyses were performed in ten patients with non-resectable hepatic malignancies prior to SIRT and 1 h and 1 week after therapy.

Materials and methods

Patients

Ten patients with a mean age of 74 years (range 68–81) were recruited who received SIRT because of hepatic tumors (nine males with hepatocellular carcinoma and one female with intrahepatic angiosarcoma). Two of the patients had lymph node metastases, two lung metastasis, one a metastasis in the adrenal gland and one in the pancreas, but none of them had bone metastases. The patient with angiosarcoma had Child-Pugh score 0 (= no liver cirrhosis), the remaining patients score A. None of the patients had previously been transplanted, had received immunosuppressive drugs or treatment with sorafenib or radiotherapy within the last year or suffered from autoimmune disease. The mean administered activity of ^{90}Y was 2.9 GBq (range 1.0–6.4), the mean target volume dose was 114 Gy (104–119). Measurement of DNA lesions and of cellular immunity was performed immediately prior to therapy (day 0) and 1 h and 1 week post therapy. For comparison, PHA-induced proliferation was determined in 177 matched healthy controls.

Assessment of lymphocyte function

To measure lymphocyte proliferation, the highly sensitive lymphocyte transformation test (LTT) was chosen, which determines the uptake of ^{3}H thymidine by proliferating cells and which has been the gold standard for decades [7, 8, 10, 11]. To assess cytokine production, the ELISpot method was applied, which determines cytokine production on a single cell level and which can reliably quantify effects of irradiation on immune function [12, 20–22]. PHA was used to stimulate lymphocyte proliferation and secretion of IFN-γ. Of note, PHA-induced lymphocyte proliferation is commonly determined to assess the general T cell function, e.g. when suspecting immunodeficiency [23]. The LTT and ELISpot have recently been described in detail [12]. In brief, 50,000 of freshly isolated, vital PBMC were incubated with and without PHA for 4 days. To assess proliferation, the cultures were labeled with 37 kBq ^{3}H thymidine per culture and the incorporated radioactivity was quantified by liquid scintillation counting. To determine IFN-γ secretion,

200,000 vital PBMC were grown with and without PHA stimulation. After 3 days of cell culture, spot formation was analyzed by an ELISpot plate reader.

Cryopreservation and thawing of cells

After performing proliferation and ELISpot assays with the freshly isolated PBMC, the residual cells were frozen to test them in one run for DNA lesions. A pellet of 10 million PBMC per vial was frozen with 1 mL freezing medium containing 740 µL RPMI 1640, 160 µL fetal calf serum (FCS, Biochrom, Berlin, Germany), 100 µL dimethylsulfoxide (DMSO, Serva, Heidelberg, Germany), 20 U/mL heparin (Liquimin, La Roche, Grenzach Wyhlen, Germany) and 10 µg/mL DNAse (Boehringer, Mannheim, Germany). The vials were cooled down in a freezing box (Mr Frosty™ Freezing Container, Nalgene, Neerijse, Belgium) and stored thereafter in liquid nitrogen.

To thaw the cells, the vials were put into a water bath with 37 °C until the cell suspension was partly thawed. The cell suspension was then washed once with thawing medium (freezing medium without DMSO) and twice with cell culture medium [RPMI 1640, 1% penicillin/streptomycin, 200 µg/mL L-glutamine and 10% pooled human serum (Transfusion Medicine, University Hospital, Essen, Germany)]. Thereafter, the cells were adjusted to 1 million of vital PBMC per mL with PBS.

Assessment of DNA lesions

Determination of DNA lesions was carried out according to the manufacturer's instructions using the γH2AX immunofluorescence staining kit (AKLIDES® Nuk Human Lymphocyte Complete, Medipan, Berlin, Germany) and anti-53BP1 as an additional antibody (Novus Biologicals Abingdon, United Kingdom) [24]. Thawed PBMC (50,000 vital cells diluted with 50 µL PBS) were pipetted onto 6-well sialinized glass slides, the cells were allowed to settle for 10 min and then they were fixed with 50 µL 2% paraformaldehyde for another 15 min. Slides were washed three times for 10 min each in PBS. Thereafter, permeabilization with 0.2% Triton X-100 was performed for 5 min at 4 °C and the slides were washed three times with PBS containing 1% bovine serum albumin (PBS/BSA). For co-immunostaining anti-γH2AX mouse monoclonal antibody and anti-53BP1 rabbit polyclonal antibody were diluted 1:200 in 1% PBS/BSA and the slides were incubated for 1 h at room temperature with 25 µL of each antibody. After a further washing step with 1% PBS/BSA, 25 µL of 1:500 diluted Alexa Fluor 488 goat anti-mouse IgG (Invitrogen, Karlsruhe, Germany) and Alexa Fluor 647 goat anti-rabbit IgG (Invitrogen) were added for 1 h at room temperature. After a final washing step with PBS, cells were covered with 4,6′-diamidino-2-phenylindole (DAPI) containing mounting medium. Finally, γH2AX and 53BP1 foci were analyzed using the fully automated AKLIDES® system (Medipan) allowing an automated evaluation of fluorescence microscope images, as described previously [24, 25]. For each well at least 100 cells were selected randomly and the median value of γH2AX and 53BP1 foci per well was used for further analysis.

Statistical analysis

Data on lymphocyte proliferation were given as counts per minute (CPM), representing the uptake of ^{3}H thymidine, and ELISpot data as spot numbers per cell culture. Increment values of both parameters were generated, which means that the background reaction (without stimulation) was subtracted from the reaction toward PHA. The quotient of 53BP1 and γH2AX foci was calculated as a ratio of median foci numbers for each sample. If not otherwise stated, mean and standard error of the mean (SEM) were indicated. Wilcoxon matched pairs test was used to compare data prior to therapy (day 0) with data 1 h and 1 week after therapy, respectively. Correlation analyses were performed by Spearman test. Analyses were performed two-sided and considered significant at $p < 0.05$. Data were analyzed using GraphPad Prism software version 5.03 (La Jolla, CA, U.S.A.) or IBM SPSS Statistics version 22 (Armonk, NY, U.S.A.), respectively.

Results

In patients with non-resectable hepatic malignancies the number of γH2AX foci was 3.5- and 3.1-fold increased 1 h and 1 week after SIRT, respectively, as compared to baseline (1.58 ± 0.28 and 1.37 ± 0.15 vs. 0.44 ± 0.13 foci per cell, $p < 0.005$ each) (Fig. 1a). Similarly, the number of 53BP1 foci was 3.2- and 3.8-fold increased 1 h and 1 week after therapy (0.40 ± 0.07 and 0.46 ± 0.07 vs. 0.12 ± 0.04 foci per cell, $p < 0.01$ each) (Fig. 1b). The quotient of 53BP1 and γH2AX foci (53BP1/γH2AX) slightly increased over time (0.28 ± 0.06, 0.31 ± 0.06 and 0.34 ± 0.03, Fig. 1c). We observed that γH2AX foci at baseline tended to correlate with those 1 week after SIRT ($r = 0.47$, $p = 0.17$) and that 53BP1 foci at baseline significantly correlated with those 1 week after SIRT ($r = 0.69$, $p = 0.03$, Fig. 1d). Thus, baseline levels of double-strand breaks, especially of 53BP1 foci, could determine susceptibility to subsequent damage after SIRT. Moreover, correlation between γH2AX and 53BP1 foci reached statistical significance 1 h ($r = 0.64$ and $p = 0.048$) and 1 week after SIRT ($r = 0.87$ and $p = 0.001$) (Fig. 2) but not prior to therapy ($r = 0.58$ and $p = 0.09$).

Already prior to SIRT proliferative responses to PHA were reduced in six out of ten patients as compared to 177

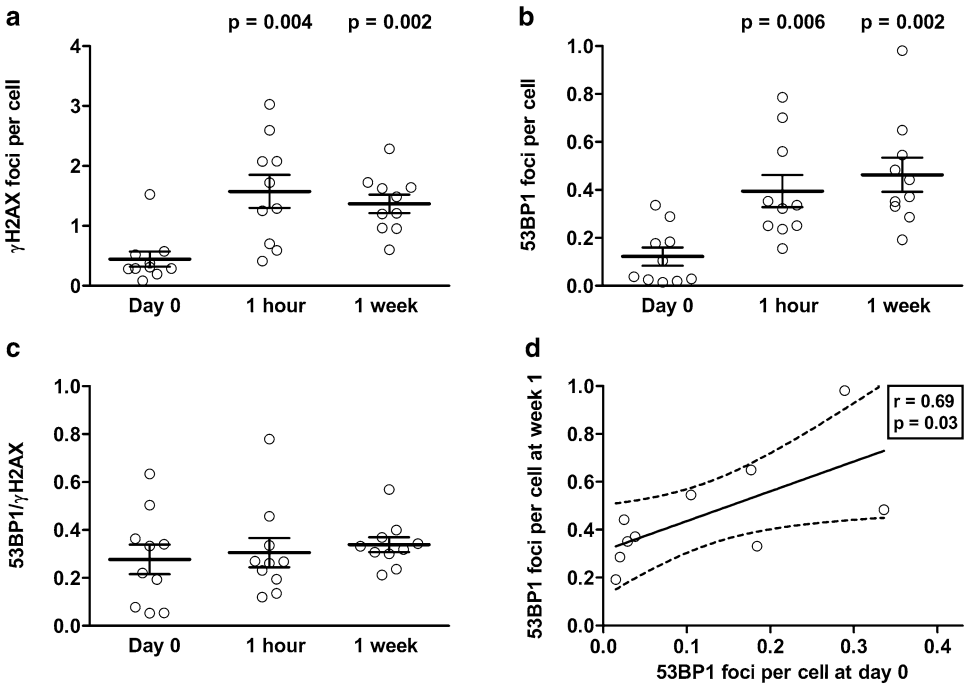

Fig. 1 DNA foci in ten patients with hepatic malignancies receiving selective internal radiotherapy. γH2AX foci and 53BP1 foci were determined as a measure of DNA double strand breaks. Wilcoxon matched pairs test was used to compare data prior to therapy (day 0) with data 1 h and 1 week after therapy, respectively. Mean and standard error of the mean (SEM) are indicated by horizontal lines (**a**–**c**). **d** Shows results of a Spearman correlation analysis between 53BP1 foci at day 0 and week 1 after therapy. The continuous line represents the regression line, the broken lines the 95% confidence interval

healthy controls (Fig. 3a). After SIRT we observed a further decrease of PHA-induced lymphocyte proliferation. 1 h and 1 week after SIRT, PHA-induced proliferation was below the normal range in eight and nine out of ten patients, respectively. Moreover, PHA-induced IFN-γ production significantly decreased at week 1 after SIRT ($p=0.03$) (Fig. 3b).

Prior to therapy, there was a highly significant, inverse correlation between lymphocyte proliferation after PHA stimulation and the quotient 53BP1/γH2AX ($r=-0.94$, $p<0.0001$) (Fig. 4a). Of note, this phenomenon occurred irrespective of SIRT. In those four patients with normal response to PHA, the quotient 53BP1/γH2AX was lowest (<0.2). 1 h and 1 week after SIRT a correlation between lymphocyte proliferation and the quotient 53BP1/γH2AX could no longer be detected ($r=-0.05$ 1 h after SIRT and $r=0.19$ at week 1). 1 h after SIRT, proliferative responses were inversely correlated with γH2AX foci ($r=-0.65$, $p=0.049$) (Fig. 4b). Prior to therapy and 1 h after therapy proliferative responses were inversely correlated with 53BP1 foci ($r=-0.66$, $p=0.044$ at both time points) (Fig. 4c, d). 1 week after SIRT, however, lymphocyte proliferation did no longer correlate significantly with γH2AX foci or 53BP1 foci but showed a tendency for an inverse correlation. Thus, 1 h after therapy a decrease in lymphocyte proliferation correlated with an increase in γH2AX and 53BP1 foci.

It could be assumed that γH2AX and 53BP1 foci correlated with the administered radioactivity and that impaired proliferation results as a consequence. Therefore, correlation analyses with the activity were performed (Table 1). However, none of these analyses yielded statistically significant results. 1 h after SIRT the activity tended to correlate with γH2AX foci ($r=0.33$, $p=0.35$) and with 53BP1 foci ($r=0.47$, $p=0.17$) and 1 week after SIRT it tended to correlate with 53BP1 foci and with the quotient 53BP1/γH2AX ($r=0.53$, $p=0.12$ and $r=0.38$, $p=0.28$, respectively). Similarly, the correlation between proliferation and activity was analyzed. There was a trend towards inverse correlation 1 week after SIRT ($r=-0.32$, $p=0.37$). Thus, according to these statistical analyses it appears unlikely that altered proliferation is solely a consequence of the administered activity.

Consistent with the data on PHA-induced lymphocyte proliferation, PHA-induced IFN-γ production tended to correlate inversely with the quotient 53BP1/γH2AX at day 0, γH2AX foci 1 h after SIRT and 53BP1 foci at day 0 and 1 h after therapy, respectively. Thus, in addition to the decrease of lymphocyte proliferation IFN-γ production also decreased when γH2AX and 53BP1 foci increased.

γH2AX and 53BP1 foci also correlated with age. 1 h after SIRT, there was a positive correlation between γH2AX foci and age ($r=0.78$, $p=0.008$) and between 53BP1 foci and age ($r=0.73$, $p=0.02$), i.e., older patients had increased numbers of foci after SIRT (Table 1; Fig. 5a, b). 1 h after SIRT, PHA-induced lymphocyte proliferation inversely correlated with age ($r=-0.76$, $p=0.01$, Table 1; Fig. 5c). Thus, in older patients, larger numbers of γH2AX and 53BP1 foci and decreased lymphocyte proliferation were observed.

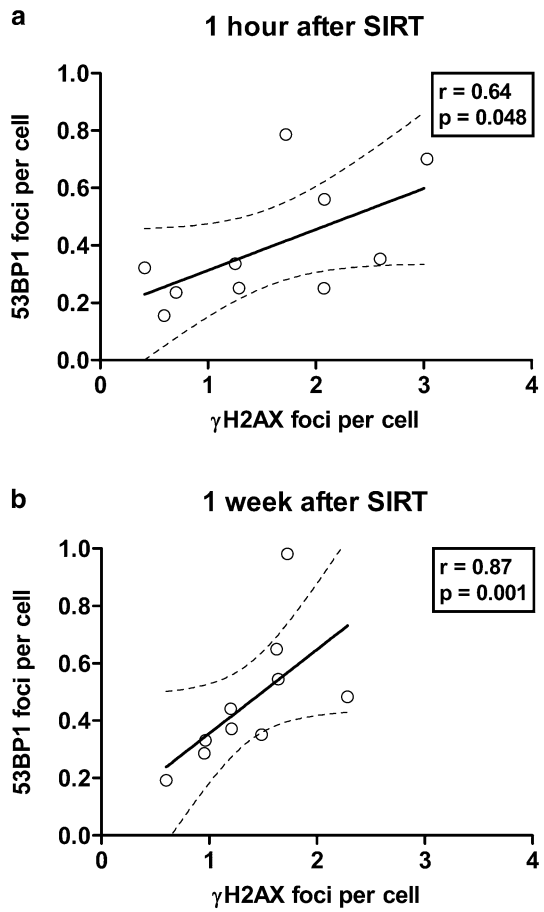

Fig. 2 Spearman correlation analysis of γH2AX and 53BP1 foci in ten patients with hepatic malignancies. Positive correlations were observed **a** 1 h and **b** 1 week at after selective internal radiotherapy. The continuous line represents the regression line, the broken lines the 95% confidence interval

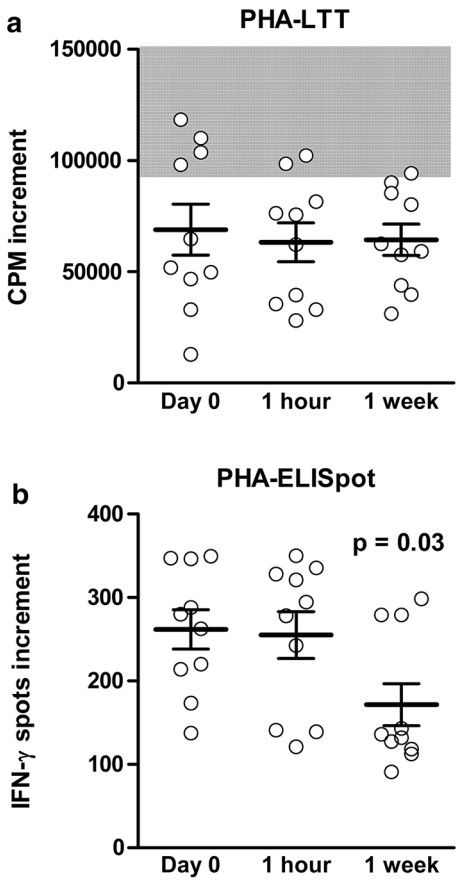

Fig. 3 Lymphocyte responses in ten patients with hepatic malignancies. Lymphocytes were stimulated by the mitogen PHA and **a** proliferation was determined by lymphocyte transformation test (LTT) and **b** IFN-γ production by ELISpot. Data are given as counts per minute (CPM) of ^{3}H thymidine uptake or as spot numbers per cell culture. Increment means that the background reaction (without stimulation) was subtracted from the reaction toward PHA. Wilcoxon matched pairs test was used to compare data prior to selective internal radiotherapy (day 0) with data 1 h and 1 week after therapy, respectively. Mean and standard error of the mean (SEM) are indicated by horizontal lines. The gray shaded area displays the normal range which was defined in 177 healthy controls. The threshold is the 5% percentile of cellular responses as determined in these controls

Discussion

The current study is the first analyzing in a clinical setting how SIRT affects markers of DNA DSBs and how these DSBs correlate with cellular immune responses. Because the use of radiopharmaceuticals for cancer therapy increases, it is important to elucidate its effects on the immune system; which may be critical to manage toxicity. Furthermore, a possible combination of SIRT with other treatment modalities, such as immune-checkpoint inhibitors, makes it essential to understand the effect of radiotherapy on the immune system. According to a publication by Napolitano et al. [26] PD-1 positive regulatory T cells were predictive of responses to neoadjuvant short-course preoperative radiotherapy in rectal cancer patients. In detail, they described that patients with a good response to radiotherapy showed a decrease in the percentage of CD4+/CD25hi+/FOXP3+/PD-1 + Tregs; whereas those with a poor response showed an increase of these Tregs. Similarly, changes in numbers of cells expressing PD-1 after SIRT could impact on the outcome.

Since the liver is a well-perfused organ with a mean total hepatic blood flow of approximately 1 L/min [27–29], the whole blood is irradiated during its passage through the liver circulation. Considering the half-life time of ^{90}Y (64.1 h) and of the circulating lymphocytes (> 150 days) [30], it is very likely that lymphocytes are irradiated several times. The dose to lymphocytes 1 h after SIRT should be in the range of 130–150 mGy. This rough estimation is based on the following considerations: The average radiation dose of the total liver including the malignant tumors was 114 Gy (cumulative dose). The range of the beta particles emitted

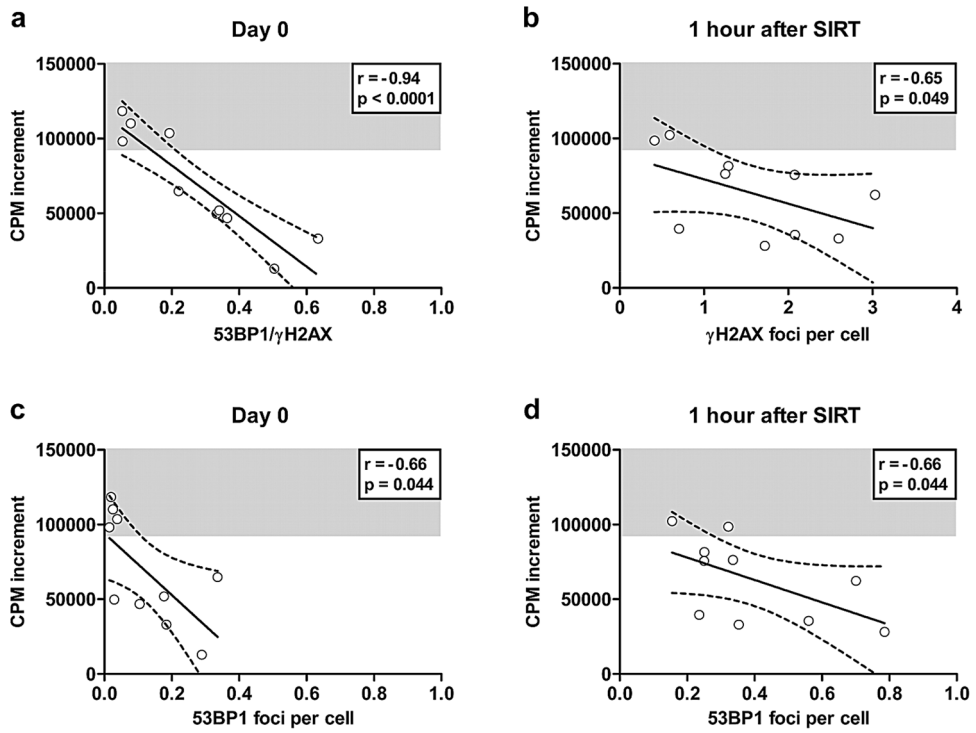

Fig. 4 Spearman correlation analysis of lymphocyte proliferation and DNA foci in ten patients with hepatic malignancies. Lymphocyte proliferation after stimulation with phythohemagglutinin (PHA) inversely correlates **a** with the quotient 53BP1/γH2AX prior to selective internal radiotherapy (SIRT) (day 0), **b** with γH2AX foci 1 h after therapy, **c** with 53BP1 foci at day 0 and **d** with 53BP1 foci 1 h after therapy. Data are given as counts per minute (CPM) of ^{3}H thymidine uptake. Increment means that the background reaction (without stimulation) was subtracted from the reaction toward PHA. The continuous line represents the regression line, the broken lines the 95% confidence interval. The gray shaded area displays the normal range which was defined in 177 healthy controls. The threshold is the 5% percentile of cellular responses as determined in these controls

by ^{90}Y is large—up to 11 mm [2]—and, therefore, the dose rate in solid liver tissue and intrahepatic blood is almost the same. In healthy individuals the blood volume in the liver is approximately 10% of the whole body blood volume under normal conditions [31]. The total blood volume in the (cirrhotic) liver including the metastases is similar to that of a healthy person. This assumption is reasonable since the total blood volume in patients with liver cirrhosis is decreased [32] and on the other hand additional blood volume in the tumors must be considered [1]. The dose 1 h after SIRT was calculated according to the law for radioactive decay, considering the half-life of ^{90}Y.

Following exposure to ionizing radiation, cellular molecules such as the DNA undergo oxidative damage through direct interaction with radiation or indirectly via free radicals generated after water radiolysis [33]. One form of DNA damage is DNA DSB which can be monitored by counting the accumulation of DNA DSB markers. We observed that in the vital PBMC of patients with hepatic malignancies numbers of γH2AX and of 53BP1 foci were more than threefold larger ($p < 0.01$) 1 h and 1 week after SIRT than at baseline. Already at baseline, however, DNA DSBs were more abundant than published in healthy controls (0.03 γH2AX foci per cell) [34].

Effects of SIRT on cellular in vitro immune responses were described thoroughly in a recent paper [12]. In this previous study, we found that after administration of the beta emitter ^{90}Y into the liver lymphocyte proliferation and the capability of PBMC to produce the inflammatory cytokine IFN-γ were reduced as early as 1 h after treatment and kept on decreasing at day 2, showing the weakest cellular reaction at day 7. 1 month after SIRT (day 28) we could already observe a recovery. For this reason, we chose to analyze the DNA damage response 1 h after therapy and at day 7. Of note, impairment of lymphocyte function is not restricted to SIRT but was also observed after treatment with the radiolabeled somatostatin analogue yttrium-90 DOTA-d-Phe(1)-Tyr(3)-octreotide (DOTATOC) [21], after conventional radiotherapy [35] or after high dose chemotherapy [36].

The highly significant correlation between lymphocyte proliferation and the quotient 53BP1/γH2AX ($r = -0.94$, $p < 0.0001$) appears as an important finding. To the best of our knowledge, the significance of this quotient has not yet been defined. As 53BP1 foci occur later in the double

Table 1 Correlation of DNA foci and lymphocyte function with administered activity and age

Parameter	Date	Activity		Age	
		r	*p*	*r*	*p*
γH2AX	D0	0.12	0.75	0.30	0.41
γH2AX	D1	0.33	0.35	**0.78****	**0.008**
γH2AX	D7	0.21	0.56	−0.12	0.73
53BP1	D0	−0.04	0.91	0.00	1.00
53BP1	D1	0.47	0.17	**0.73***	**0.02**
53BP1	D7	0.53	0.12	−0.01	0.97
γH2AX	D1–D0	0.54	0.11	**0.71***	**0.02**
γH2AX	D7–D0	0.42	0.23	−0.22	0.55
53BP1	D1–D0	0.02	0.96	−0.21	0.56
53BP1	D7–D0	0.28	0.43	0.09	0.81
PHA	D0	0.28	0.43	0.45	0.19
PHA	D1	−0.19	0.60	**−0.76***	**0.01**
PHA	D7	−0.32	0.37	−0.58	0.08
PHA	D1–D0	−0.10	0.78	**−0.64***	**0.046**
PHA	D7–D0	−0.42	0.23	**−0.68***	**0.03**

Spearman correlation analysis was performed in ten patients with hepatic malignancies receiving SIRT. The analysis considered γH2AX and 53BP1 foci as markers of DNA double-strand breaks, proliferative responses to PHA as a measure of lymphocyte function (counts per minute increment), administered activity (GBq) and age (years). Prior to therapy (D0), 1 h after therapy (D1) and 1 week after therapy (D7) correlation coefficients *r* and the respective *p* values were determined. Furthermore, changes as compared to baseline (D1–D0 and D7–D0) were considered. Significant results to a two-tailed Spearman analysis are shown in bold (*$p < 0.05$, **$p < 0.01$)

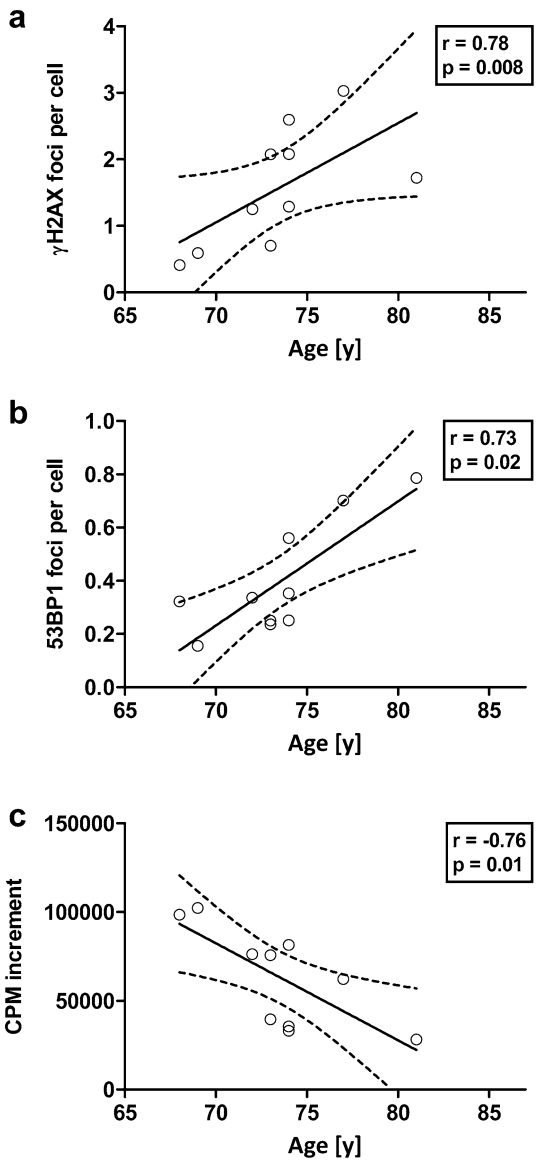

Fig. 5 Spearman correlation analysis of DNA foci or lymphocyte function and age in ten patients with hepatic malignancies. 1 h after selective internal radiotherapy, there was a significant, positive correlation between **a** γH2AX foci and age and **b** 53BP1 foci and age. Furthermore, 1 h after therapy there was an inverse correlation between lymphocyte function and age (**c**). Lymphocyte function was determined as proliferative response to PHA, given as counts per minute (CPM) of ^{3}H thymidine uptake. Increment means that the background reaction (without stimulation) was subtracted from the reaction toward PHA. The continuous line represents the regression line, the broken lines the 95% confidence interval

strand repair pathway than γH2AX foci we suggest to use this quotient as a measure of the course of DNA repair. The inverse correlation between lymphocyte proliferation and the quotient 53BP1/γH2AX at baseline may be interpreted as an impairment of lymphocyte proliferation which occurs due to ongoing DNA repair. The presence of unrepaired double-strand breaks [37] or the triggering of cell cycle arrest [38, 39] could both be reasons why lymphocytes did not proliferate adequately. Most likely, the liver malignancy per se had a dominant effect on lymphocyte function; which may be mediated by higher DNA instability (and repair rate) in six out of ten patients. In these patients proliferative responses to PHA were also below the normal range, indicating a generally impaired T cell function.

In addition, age could be identified as a factor positively correlated with γH2AX and 53BP1 foci 1 h after SIRT, i.e., older patients had increased numbers of foci. Most likely, the decreased efficiency of DSB repair pathways in aged cells as reported in several studies [40–42] lead to an accumulation of DNA lesions in the first hour after SIRT. 1 h after SIRT, PHA-induced lymphocyte proliferation correlated inversely with age. Thus, in older patients a delayed repair capacity of DNA lesions could be the cause of decreased lymphocyte proliferation. In line with this finding, we previously reported that mitogen-induced lymphocyte proliferation after radioiodine therapy was negatively correlated with age [20]. 1 week after therapy the correlation was no longer significant, presumably due to long-term repair and/or cell apoptosis.

In conclusion, the current data indicate that in patients with hepatic tumors DNA DSBs were more abundant than published in healthy controls. Elevated baseline levels were further increased after SIRT. Moreover, in the majority of patients with hepatic tumors lymphocyte proliferation was impaired. Lymphocyte proliferation was inversely correlated especially with the quotient of 53BP1and γH2AX foci; which can be regarded as a measure of the course of DNA repair. Unrepaired DNA DSBs or cell cycle arrest due to repair may cause this impairment. The causal connection between immune function and DNA lesions needs to be further elucidated.

Acknowledgements γH2AX and 53PB1 immunofluorescence stainings were kindly performed free of charge by Caroline Eberle, Lisa Heiserich and Peter Bauer (Medipan, Berlin, Germany). This article is a partial fulfilment of requirements for the doctor's degree at the Medical Faculty, University of Duisburg-Essen, for Aglaia Domouchtsidou. The authors would like to thank Monika Huben and Martina Praast for their excellent technical assistance.

Author contributions ML, VB, SPM, PL, AD, PAH and AB contributed to the conception and design of the study. AD and JB recruited the patients and took blood samples. AD performed the cellular in vitro assays. AD, PL and ML wrote the report. All authors critically revised and approved the final manuscript.

Funding No relevant funding.

Compliance with ethical standards

Conflict of interest The authors declare that they have no conflict of interest.

Ethical approval and ethical standards The study was institutional review board approved by the ethics committee of the Medical Faculty, University Hospital Essen (approval number 09-3991), and carried out in accordance with the 1964 Helsinki Declaration.

Informed consent All participants provided written informed consent prior to their inclusion in the study.

References

1. Lewandowski RJ, Salem R (2006) Yttrium-90 radioembolization of hepatocellular carcinoma and metastatic disease to the liver. Semin Intervent Radiol 23(1):64–72
2. Kennedy AS, McNeillie P, Dezarn WA et al (2009) Treatment parameters and outcome in 680 treatments of internal radiation with resin ^{90}Y-microspheres for unresectable hepatic tumors. Int J Radiat Oncol Biol Phys 74(5):1494–1500
3. Wang LM, Jani AR, Hill EJ, Sharma RA (2013) Anatomical basis and histopathological changes resulting from selective internal radiotherapy for liver metastases. J Clin Pathol 66(3):205–211
4. Dezarn WA, Cessna JT, DeWerd LA et al (2011) Recommendations of the American Association of Physicists in Medicine on dosimetry, imaging, and quality assurance procedures for ^{90}Y microsphere brachytherapy in the treatment of hepatic malignancies. Med Phys 38(8):4824–4845
5. Salem R, Thurston KG (2006) Radioembolization with 90yttrium microspheres: a state-of-the-art brachytherapy treatment for primary and secondary liver malignancies. Part 2: special topics. J Vasc Interv Radiol 17(9):1425–1439
6. Smyth MJ, Ngiow SF, Ribas A, Teng MW (2016) Combination cancer immunotherapies tailored to the tumour microenvironment. Nat Rev Clin Oncol 13(3):143–158
7. Fridman WH, Pages F, Sautes-Fridman C, Galon J (2012) The immune contexture in human tumours: impact on clinical outcome. Nat Rev Cancer 12(4):298–306
8. Gentles AJ, Newman AM, Liu CL et al (2015) The prognostic landscape of genes and infiltrating immune cells across human cancers. Nat Med 21(8):938–945
9. Rooney MS, Shukla SA, Wu CJ, Getz G, Hacohen N (2015) Molecular and genetic properties of tumors associated with local immune cytolytic activity. Cell 160(1–2):48–61
10. Becht E, Giraldo NA, Dieu-Nosjean MC, Sautes-Fridman C, Fridman WH (2016) Cancer immune contexture and immunotherapy. Curr Opin Immunol 39:7–13
11. Foerster F, Hess M, Gerhold-Ay A, Marquardt JU, Becker D, Galle PR, Schuppan D, Binder H, Bockamp E (2018) The immune contexture of hepatocellular carcinoma predicts clinical outcome. Sci Rep 8(1):5351
12. Domouchtsidou A, Barsegian V, Mueller SP, Best J, Ertle J, Bedreli S, Horn PA, Bockisch A, Lindemann M (2018) Impaired lymphocyte function in patients with hepatic malignancies after selective internal radiotherapy. Cancer Immunol Immunother 67(5):843–853
13. Lobrich M, Rief N, Kuhne M, Heckmann M, Fleckenstein J, Rube C, Uder M (2005) In vivo formation and repair of DNA double-strand breaks after computed tomography examinations. Proc Natl Acad Sci USA 102(25):8984–8989
14. Khanna KK, Jackson SP (2001) DNA double-strand breaks: signaling, repair and the cancer connection. Nat Genet 27(3):247–254
15. Rogakou EP, Pilch DR, Orr AH, Ivanova VS, Bonner WM (1998) DNA double-stranded breaks induce histone H2AX phosphorylation on serine 139. J Biol Chem 273(10):5858–5868
16. Panier S, Boulton SJ (2014) Double-strand break repair: 53BP1 comes into focus. Nat Rev Mol Cell Biol 15(1):7–18
17. Rappold I, Iwabuchi K, Date T, Chen J (2001) Tumor suppressor p53 binding protein 1 (53BP1) is involved in DNA damage-signaling pathways. J Cell Biol 153(3):613–620
18. Zwicker F, Swartman B, Sterzing F, Major G, Weber KJ, Huber PE, Thieke C, Debus J, Herfarth K (2011) Biological in-vivo measurement of dose distribution in patients' lymphocytes by gamma-H2AX immunofluorescence staining: 3D conformal- vs. step-and-shoot IMRT of the prostate gland. Radiat Oncol 6:62
19. Gupta A, Hunt CR, Chakraborty S, Pandita RK, Yordy J, Ramnarain DB, Horikoshi N, Pandita TK (2014) Role of 53BP1 in the regulation of DNA double-strand break repair pathway choice. Radiat Res 181(1):1–8
20. Barsegian V, Müller SP, Horn PA, Bockisch A, Lindemann M (2011) Lymphocyte function following radioiodine therapy in patients with thyroid carcinoma. Nuklearmedizin 50(5):195–203
21. Barsegian V, Hueben C, Mueller SP, Poeppel TD, Horn PA, Bockisch A, Lindemann M (2015) Impairment of lymphocyte function following yttrium-90 DOTATOC therapy. Cancer Immunol Immunother 64(6):755–764
22. Barsegian V, Muller SP, Mockel D, Horn PA, Bockisch A, Lindemann M (2017) Lymphocyte function following radium-223 therapy in patients with metastasized, castration-resistant prostate cancer. Eur J Nucl Med Mol Imaging 44(2):242–246
23. Lindemann M (2014) Ex vivo assessment of cellular immune function - applications in patient care and clinical studies. Tissue Antigens 84(5):439–449

24. Buchali A, Heiserich L, Bauer P, Tregel M, Roggenbuck D, Franzen A (2017) Baseline H2AX foci, 53BP1 values and late morbidity after definitive radio-chemotherapy in head and neck carcinoma patients. J Solid Tumors 7(1):11–15
25. Goutham HV, Mumbrekar KD, Vadhiraja BM, Fernandes DJ, Sharan K, Kanive Parashiva G, Kapaettu S, Bola Sadashiva SR (2012) DNA double-strand break analysis by gamma-H2AX foci: a useful method for determining the overreactors to radiation-induced acute reactions among head-and-neck cancer patients. Int J Radiat Oncol Biol Phys 84(5):e607–e612
26. Napolitano M, D'Alterio C, Cardone E et al (2015) Peripheral myeloid-derived suppressor and T regulatory PD-1 positive cells predict response to neoadjuvant short-course radiotherapy in rectal cancer patients. Oncotarget 6(10):8261–8270
27. Greenway CV, Stark RD (1971) Hepatic vascular bed. Physiol Rev 51(1):23–65
28. Schenk WG Jr, Mc DJ, Mc DK, Drapanas T (1962) Direct measurement of hepatic blood flow in surgical patients: with related observations on hepatic flow dynamics in experimental animals. Ann Surg 156:463–471
29. Yzet T, Bouzerar R, Baledent O, Renard C, Lumbala DM, Nguyen-Khac E, Regimbeau JM, Deramond H, Meyer ME (2010) Dynamic measurements of total hepatic blood flow with Phase Contrast MRI. Eur J Radiol 73(1):119–124
30. Vrisekoop N, den Braber I, de Boer AB et al (2008) Sparse production but preferential incorporation of recently produced naive T cells in the human peripheral pool. Proc Natl Acad Sci USA 105(16):6115–6120
31. Joubert-Huebner E Kap. 6. Leber. Anatomie und Physiologie. The European Board of Cardiovascular Perfusion. http://www.kardiotechnik.org/kap_06.pdf. Accessed 8 Jan 2019
32. Van Beers BE, Leconte I, Materne R, Smith AM, Jamart J, Horsmans Y (2001) Hepatic perfusion parameters in chronic liver disease: dynamic CT measurements correlated with disease severity. AJR Am J Roentgenol 176(3):667–673
33. Azzam EI, Jay-Gerin JP, Pain D (2012) Ionizing radiation-induced metabolic oxidative stress and prolonged cell injury. Cancer Lett 327(1–2):48–60
34. Scherthan H, Hieber L, Braselmann H, Meineke V, Zitzelsberger H (2008) Accumulation of DSBs in gamma-H2AX domains fuel chromosomal aberrations. Biochem Biophys Res Commun 371(4):694–697
35. Belka C, Ottinger H, Kreuzfelder E, Weinmann M, Lindemann M, Lepple-Wienhues A, Budach W, Grosse-Wilde H, Bamberg M (1999) Impact of localized radiotherapy on blood immune cells counts and function in humans. Radiother Oncol 50(2):199–204
36. Lindemann M, Schuett P, Moritz T, Ottinger HD, Opalka B, Seeber S, Nowrousian MR, Grosse-Wilde H (2005) Cellular in vitro immune function in multiple myeloma patients after high-dose chemotherapy and autologous peripheral stem cell transplantation. Leukemia 19(3):490–492
37. Rothkamm K, Lobrich M (2003) Evidence for a lack of DNA double-strand break repair in human cells exposed to very low X-ray doses. Proc Natl Acad Sci USA 100(9):5057–5062
38. Kousholt AN, Menzel T, Sorensen CS (2012) Pathways for genome integrity in G2 phase of the cell cycle. Biomolecules 2(4):579–607
39. Fernandez-Capetillo O, Chen HT, Celeste A et al (2002) DNA damage-induced G2-M checkpoint activation by histone H2AX and 53BP1. Nat Cell Biol 4(12):993–997
40. Garm C, Moreno-Villanueva M, Burkle A, Petersen I, Bohr VA, Christensen K, Stevnsner T (2013) Age and gender effects on DNA strand break repair in peripheral blood mononuclear cells. Aging Cell 12(1):58–66
41. Seluanov A, Mittelman D, Pereira-Smith OM, Wilson JH, Gorbunova V (2004) DNA end joining becomes less efficient and more error-prone during cellular senescence. Proc Natl Acad Sci USA 101(20):7624–7629
42. Vaidya A, Mao Z, Tian X, Spencer B, Seluanov A, Gorbunova V (2014) Knock-in reporter mice demonstrate that DNA repair by non-homologous end joining declines with age. PLoS Genet 10(7):e1004511